Molecularly imprinted polymers for per-and polyfluoroalkyl substances enrichment and detection

Aicha Tasfaout, Farah Ibrahim, Aoife Morrin, Hugues Brisset, Ilaria Sorrentino, Clément Nanteuil, Guillaume Laffite, Ian Nicholls, Fiona Regan, Catherine Branger

Molecularly imprinted polymers for per- and polyfluoroalkyl substances enrichment and detection

Aicha Tasfaout[1#], Farah Ibrahim[2#], Aoife Morrin[1], Hugues Brisset[2], Ilaria Sorrentino[3], Clément Nanteuil[3], Guillaume Laffite[3], Ian A. Nicholls[4], Fiona Regan[1], Catherine Branger[2,*]

[1] *School of Chemical Sciences, National Centre for Sensor Research, Dublin City University, Glasnevin, Dublin 9, Ireland*

[2] *Université de Toulon, Laboratoire Matériaux Polymères Interfaces Environnement Marin (MAPIEM), Toulon, France*

[3] *Klearia, 61 Avenue Simone Veil, CEEI Nice Côte d'Azur - Immeuble Premium, 06200 Nice, France*

[4] *Bioorganic & Biophysical Chemistry Laboratory, Department of Chemistry & Biomedical Sciences, Linnaeus University, SE-39182 Kalmar, Sweden.*

[#] *Authors with equal contribution*

Corresponding author: branger@univ-tln.fr

Abstract

Per- and polyfluoroalkyl substances (PFAS) are highly toxic pollutants of significant concern as they are being detected in water, air, fish and soil. They are extremely persistent and accumulate in plant and animal tissues. Traditional methods of detection and removal of these substances use specialised instrumentation and require a trained technical resource for operation. Molecularly imprinted polymers (MIPs), polymeric materials with predetermined selectivity for a target molecule, have recently begun to be exploited in technologies for the selective removal and monitoring of PFAS in environmental waters. This review offers a comprehensive overview of recent developments in MIPs, both as adsorbents for PFAS removal and sensors that selectively detect PFAS at environmentally-relevant concentrations. PFAS-MIP adsorbents are classified according to their method of preparation (e.g., bulk or precipitation polymerization, surface imprinting), while PFAS-MIP sensing materials are described and discussed according to the transduction methods used (e.g., electrochemical, optical). This review aims to comprehensively discuss the PFAS-MIP research field. The efficacy and challenges facing the different applications of these materials in environmental water applications are discussed, as well as a perspective on challenges for this field that need to be overcome before exploitation of the technology can be fully realised.

Keywords Per- and polyfluoroalkyl substances (PFAS), molecularly imprinted polymers (MIPs), sensor, adsorption, environmental waters

Contents

Abbreviations

AA	Acrylic acid
AAM	Acrylamide
An	Aniline
APTES	Aminopropyltriethoxysilane
BPA	Bisphenol A
CMS	Carbon microspheres
CQD	Carbon quantum dots
CTAB	Cetyltrimethylammonium bromide
DBP	Dibutyl phthalate
2,4-D	2,4-Dichlorophenoxyacetic acid
ECH	Epichlorohydrin
ECL	Electrochemiluminescence
EGDMA	Ethylene glycol dimethylacrylate
FITC	Fluorescein 6-isothiocyanate
FTO	Fluorine-doped tin oxide
FTS	Fluorotelomer sulfonate
GC	Gas chromatography
GAC	Granular activated carbon
GCE	Glassy carbon electrode
HPLC	High performance liquid chromatography
IF	Imprinting factor
LC	Liquid chromatography
LC-MS	Liquid chromatography coupled with mass spectroscopy
LOD	Limit of detection
MAA	Methacrylic acid
MBA	N,N′-Methylenebis(acrylamide)
MIP	Molecularly imprinted polymer
MMIP	Magnetic molecularly imprinted polymers

MS	Mass spectrometry
MS/MS	Tandem mass spectrometry
MSN	Mesoporous silica nanoparticles
MTAC	Methacryloyloxyethyl trimethyl ammonium chloride
MWCNT	Multi-walled carbon nanotubes
NIP	Non-imprinted polymer
NP	Nanoparticle
NTA	Nanotube arrays
NF	Nanoflake (arrays)
PANI	Polyaniline
PCP	Phencyclidine
oPD	o-Phenyldiamine
PEC	Photoelectrochemical
PFAS	Per- and polyfluoroalkyl substances
PFBA	Perfluorobutanoic acid
PFBS	Perfluorobutanesulfonic acid
PFC	Per- and polyfluoroalkyl compounds
PFDA	Perfluorodecanoic acid
PFDoA	Perfluorododecanoic acid
PFHxA	Perfluorohexanoic acid
PFHpA	Perfluoroheptanoic acid
PFHSK	Perfluorohexanesulfonic acid potassium salt
PFNA	Perfluorononanoic acid
PFOA	Perfluorooctanoic acid
PFOS	Perfluorosulfonic acid
PFOSF	Perfluorooctanesulfonyl fluoride
PFPeA	Perfluoropentanoic acid
PFTeDA	Perfluorotetradecanoic acid
PFUnA	Perfluoroundecanoic acid
PL	Photoluminescence
PLMIP	Photoluminescent molecularly imprinted polymer
POF	Plastic optical fiber
PPy	Poly-pyrrole
Py	Pyrrole
QD	Quantum dots
RSD	Relative standard deviation
SDBS	Sodium dodecylbenzene sulfonate
SDS	Sodium dodecyl sulfate
SPE	Screen-printed electrode or Solid phase extraction
SPR	Surface plasmon resonance
TEOS	Tetraethoxysilane
TFMAA	2-(Trifluoromethyl) acrylic acid
TRIA	Trimethylolpropane triacrylate
TRIM	Trimethylopropane trimethacrylate
UHPLC	Ultra-high performance liquid chromatography
VBT	(4Vinylbenzyl)thymine
VPy	Vinylpyridine
WHO	World health organization

1. Introduction

Per- and polyfluorinated alkyl substances (PFAS), also known as per- and polyfluorinated compounds (PFC), have been used for decades in a range of applications like firefighting foams, non-stick cookware

and water and stain-resistant clothing [1,2]. They make up a large group of over 4700 artificial chemicals, to which humans are exposed daily, in soil, water and air, and are of significant health concern. Epidemiological studies show that PFAS constitute a danger to the endocrine and reproductive systems [1].

The PFAS class of compounds covers fully (per-) or partly (poly-) fluorinated aliphatic compounds in which at least one carbon atom is fully fluorinated. The general structure of the perfluorinated aliphatic compounds contain the moiety C_nF_{2n+1}—*R*, where *n* is the number of carbon atoms, while R refers to the functional group (carboxylate, sulfonate, phosphonate…etc.) [3]. Amongst PFAS, perfluorooctane sulfonate (PFOS) and perfluorooctanoic acid (PFOA) (Table 1) have drawn particular attention and generated regulatory concerns in recent years. These are the most frequently detected PFASs in the environment [4,5]. They are highly resistant to thermal, biological and chemical decomposition and photolysis and thus highly persistent [6,7]. They have been listed as persistent organic pollutants by the Stockholm Convention and in the reduction plan by the US Environment Protection Agency [8,9]. The World Health Organization (WHO) has recently set maximal values of 0.4 $\mu g.L^{-1}$ and 4 $\mu g.L^{-1}$ for PFOS and PFOA respectively in drinking water intended for human consumption [10].

The C-F bond is highly polar and one of the strongest covalent bonds (544 $kJ.mol^{-1}$), which renders this class of chemical highly resistant to complete degradation [11]. Moreover, the low polarizability of the fluorine atom imparts hydrophobic and lipophobic properties, while the terminal functional R group gives them chemical and thermal stability [12]. Additionally, most PFAS containing long per-fluorinated chains exhibit amphiphilic properties, owing to the hydrophobic tail and the hydrophilic functional group. This contributes to their high solubility in water and absorption in soil, which paired with their high stability and resistance to degradation, leads to severe risks of pollution of natural resources and persistence in these environments [13]. Furthermore, PFAS are most likely to be absorbed by the human body through oral ingestion, as they persist in drinking water, transferred to food through non-stick cookware and certain cleaning products, and sometimes even found in food packaging [1,2].

Table 1. *Name, chemical structure and acronym of several PFASs, including PFOS and PFOA (n = 8).*

Name	Structure	Acronym

Perfluoroalkyl carboxylic acid (PFCA)	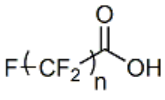	n = 4, PFBA;
		n = 5, PFPA;
		n = 6, PFHxA;
		n = 7, PFHpA;
		n = 8, PFOA;
		n = 9, PFNA;
		n = 10, PFDA;

		n = 11, PFUnA; n = 12, PFDoA

Perfluoroalkyl sulfonic acid (PFSA)	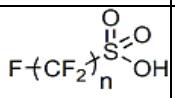	n = 4, PFBS;
		n = 5, PFPS;
		n = 6, PFHxS;
		n = 7, PFHpS;
		n = 8, PFOS

Perfluoroalkyl phosphonic acid (PFPA)	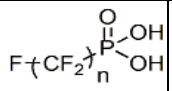	n = 6, PFHxPA;
		n = 8, PFOPA;
		n = 10, PFDPA

Perfluoroalkane sulphonamide (PFASA)	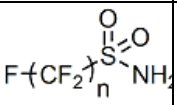	n = 4, FBSA;
		n = 6, FHxSA;
		n = 8, FOSA

PFAS consequences on human health have been getting considerable attention [14]. Toxicological studies usually tend to focus on PFOS and PFOA given their extensive use in various industries in the past and present. PFAS have been classified as endocrine disruptors, as animal studies showed that they may alter cholesterol metabolism and thyroid levels leading to severe conditions in humans [1,2,15]. More recent studies investigate the relationship between exposure to PFAS in general and abnormal ovarian functions, decline in fertility and risks of cancer in the reproductive system [1,15], although there is not enough evidence to confirm a causal relationship. In addition, some toxicological studies have shown that long-chain perfluoroalkyl acids might behave additively or interact synergistically or antagonistically when found in mixtures depending on the compounds in question, their dose levels, and ratios in the mixture [14].

Therefore, there have been many efforts to analyse these emerging contaminants in the environment, especially for drinking water and the food industry. Traditional methods used for the detection of PFAS are liquid chromatography (LC) and gas chromatography (GC) coupled with either mass spectrometry (MS) or tandem mass spectrometry (MS/MS). However, these commonly used techniques usually require a pre-treatment step based on liquid-liquid extraction or solid phase extraction (SPE). Moreover, they have some inherent disadvantages and limitations that can limit their use for the monitoring of PFAS: for example the cost, the usage of large amounts of solvent, the risk of contamination in the different steps and the interference of other compounds present in complex media that could falsify the results. Molecularly Imprinted Polymers (MIPs) appear to be an attractive alternative to overcome these shortcomings. Indeed, they can be used as selective absorbents for an efficient sample processing or as recognition elements in the

design of chemical sensors. MIPs in general represent highly selective receptor materials and are designed to bind a specific analyte through specific imprints, which can be used either as recognition element in sensors or for molecular separations by selective sorption [16].

The MIP synthesis technique consists of co-polymerising one or multiple functional monomers and a cross-linker around a template which is the target of interest (Figure 1). Once the template is removed, vacant imprinted binding cavities are generated that retain the conformation, the complementary functionality, and the size of the template. Therefore, MIPs exhibit strong affinity and high specificity for the target molecules, compared to their non-imprinted homologues (NIPs) which omit the template molecule during polymerization. The non-covalent approach is the most widespread across research published about MIP systems thanks to its simplicity and the convenience of using readily available functional monomers. In this technique, the target molecule interacts with the monomers through interactions including hydrogen bonding, van der Waals forces, $\pi-\pi$ interactions, and/or hydrophobic or ionic bonds. Hence, the selection of suitable monomers able to evolve good and stable interactions with the template is a crucial step in this approach in order to achieve a successful imprinting of the target [17].

Furthermore, the most common kind of MIPs reported in the literature are highly cross-linked polymers. They benefit from inherently high mechanical stability and robustness in a wide range of temperatures, pHs and solvents and can be prepared in varying types of formats and supports [18,19]. As a result, MIPs are extensively used in many environmental applications such as selective adsorbents for sample pretreatment [20], sensors for the selective detection of the target analyte [21] and catalysis [22]. In this review, the role, and the applications of MIPs in the enrichment and detection of PFAS in varied environmental matrices~~water~~ are investigated across the recently published literature, as they remain a relatively new technology in this field.

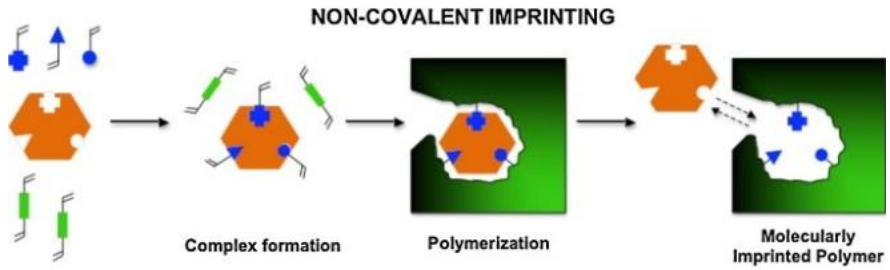

Fig. 1. Schematic representation of the synthesis of a MIP (Adapted from [23], Reprinted–with permission from Elsevier, Copyright 2012).

2. MIPs as selective adsorbents for PFAS

Various adsorbents such as granular activated carbon (GAC), powder activated carbon (PAC), resins, ion exchange polymers, alumina, boehmite and clay minerals have been used in order to extract and to detect

PFAS [24–26]. However, these materials have no selectivity for PFAS and in complex media several other compounds can be extracted as well which lowers the adsorption efficiency and distorts the results. Molecularly imprinted polymers appear to be an attractive material to allow selective extraction of PFAS.

2.1. Preparation of adsorbents

Table 2 lists the MIPs prepared for use as adsorbents for PFAS, specifying their compositions, preparation methods and performances. As far as MIPs are expected to be used as adsorbents, the desired format is usually that of particles. This format can be obtained directly through precipitation polymerization or surface imprinting technology. Bulk polymerization is easier to implement but requires the grinding and sieving of the MIPs to obtain non-monolithic polymers. For example, Deng and co-workers investigated PFOS-MIP adsorbents that were synthesized by bulk copolymerization of 4-vinylpyridine (4-VPy) as functional monomer with either trimethylolpropane triacrylate (TRIA) or ethyleneglycol dimethacryate (EGDMA) as cross-linkers in presence of PFOA or PFOS as templates [27]. Different molar ratios of PFOA/monomer/cross-linker were tested and it was noticed that the adsorbent prepared using PFOA as a template showed the highest sorption capacity. This was potentially attributed to the higher water solubility of PFOA than that of PFOS as well as the electrostatic interaction in the low pH conditions used for the sorption experiments. Cao and co-workers prepared MIP particles for PFOA by precipitation polymerization [28]. They optimized the nature of the functional monomer by using several commercial monomers that are commonly used for MIP synthesis, including acrylic acid (AA), acrylamide (AAM), 2-VPy and 4-VPy. They included 2-(trifluoromethyl) acrylic acid (TFMAA) in their study to provide additional fluorine-fluorine interaction between the functional monomer and the template. Among all tested monomers, AAM gave the MIP with the highest adsorption capacity, possibly because of the hydrogen bonding between the amide group of AAM and the carboxylic acid group of PFOA. Cao and co-workers further used TFMAA and 4-VPy as binary functional monomers and PFOA as template for preparing MIPs for PFOA and PFOS removal by precipitation polymerization (Figure 2) [29]. The presence of TFMMA in addition to AAM in the binary functional monomer MIPs enhanced their adsorption capacities compared to AAM based-MIPs due to the additional fluorine–fluorine interactions provided [28].

In another approach, Yu and co-workers used chitosan to prepare MIP adsorbents for the selective removal of PFOS from aqueous solutions [30]. Chitosan is a linear natural polymer that these authors cross-linked with epichlorohydrin (ECH) in a two-step procedure. During the second step, which corresponds to the MIP preparation, the effect of the pH of the solution was studied. It was found that the optimal MIP adsorbents were imprinted in PFOS solution at pH 3 where the electrostatic attraction between the sulfonic group in PFOS and the protonated amino groups in the chitosan molecules is favoured.

In an original approach, Yan and co-workers prepared two molecularly imprinted phenolic resin adsorbents for dispersive solid-phase extraction using a portable syringe filter [31,32]. The device was combined with LC-MS/MS. An analytical method was established for the rapid and selective extraction and determination of long-chain PFCs in food samples (milk and pork). PFNA or perfluorotetradecanoic acid (PFTeDA) were used as templates, phenolic compounds as monomers, glutaraldehyde as cross-linking agent and polyethylene glycol-6000 as the porogen.

The surface imprinting technique was developed to enhance the mass transfer rate and increase the accessibility of the recognition sites [33]. For that purpose, the surface of particles (usually inorganic in nature) is covered with an imprinted layer to provide core-shell type particles. Several kinds of particles were investigated to prepare MIP adsorbents for PFASs. Du and co-workers employed mesoporous silica nanoparticles (MSNs) as carriers to prepare core–shell structural MSNs/MIPs to separate and enrich PFOS in water samples [34]. Cao and co-workers prepared surface imprinted MIPs using multi-walled carbon nanotubes (MWCNTs) as supporting materials [35]. MWCNTs were selected due to their interesting properties such as their large surface area, their highly porous and hollow structure, their high density of π-electrons, and their ease of chemical modification. They used PFOA as template and AAM as functional monomer and reproduced the same protocol used to prepare their conventional AAM based-MIP previously described [28].

The development of magnetic molecularly imprinted polymers (MMIPs) to remove PFOS has attracted attention from Du and co-workers since they can provide superparamagnetic materials [36]. Indeed, these superparamagnetic nanoparticles can be easily separated and thus, the target molecules can be extracted rapidly. In this context, they synthesized MMIPs using PFOS as a template molecule on the surface of functionalized Fe_2O_3 nanoparticles (Figure 3) [36].

In the same perspective, Lin et *al.* constructed a superparamagnetic core-shell MIP via self-polymerization of dopamine around PFOS and immobilization onto Fe_3O_4 substrate [37]. The same group designed a MIP adsorbent by surface imprinting on carbon microspheres (CMSs) as carrier [38]. CMSs were chosen because they are stable in acidic conditions and their mechanical stability is also good. An amine group was introduced onto the surface of the CMSs by silanization to increase the reactivity of the surface. They used PFOA as template and methacryloyloxyethyl trimethyl ammonium chloride (MTAC) and TFMAA as binary functional monomers to include two different kinds of binding forces, which provided good binding selectivity to the template. The tertiary amine groups of the MTAC monomer and the carboxyl groups in the TFMA can be easily protonated at low pH. Hence, the electrostatic interaction between the functional monomers and the PFOS played an important role in the adsorption process at acidic pH as well as the fluorine-fluorine interaction most probably involved in the adsorption.

Hu and co-workers were concerned by the destruction of harmful perfluorinated pollutants during the regeneration process of the MIPs adsorbents [39]. They combined the MIP adsorption for PFASs with TiO_2 photocatalysis in order to develop a photocatalyst to achieve selective removal of perfluorinated compounds from secondary effluents and simultaneous regeneration the polymers. The photocatalyst was prepared by surface coating of vinyl-functionalized TiO2 nanotube arrays (NTAs) with a thin MIP layer using methacrylic acid (MAA) and trimethylopropane trimethacrylate (TRIM) as functional monomer and cross-linker respectively. Wu and co-workers fabricated a similar MIP-modified TiO_2 photocatalyst using AAM and EGDMA as monomers [40].

In all studies reported, subsequent to MIP synthesis, the removal of the template and unreacted monomers was achieved by successive extraction using an organic solvent or a mixture of an organic solvent with an

187 acid or a base or pure water until no template was detected in the eluate. Therefore, no contamination with
188 PFAS template to the environment is assumed during MIP usage.

189 ***2.2. Properties/characteristics of the adsorbents***

190 PFOS and PFOA adsorption on MIPs are pH dependent. Indeed, the pH of the solution not only influences
191 the properties of the adsorbent surface but also affects the speciation of target pollutant in solution. For
192 example, PFOA ionizes in water to form a perfluorocarboxylic anion when the solution pH is above its pKa
193 value of 2.8 [41] whereas the pKa of the sulfonic group in PFOS is about -3.27 [42]. In most cases, MIPs
194 show highest removal rates for PFOS and PFOA at low pH where the functional groups present in the
195 adsorbents such as pyridine [27,29], amine [30,36] and quaternary ammonium [38] are positively charged.
196 Consequently, electrostatic attraction between the target and the MIP adsorbent dominates the adsorption
197 process. With increasing solution pH, deprotonated forms of the functional groups are sometimes formed
198 and electrostatic repulsion between the target and the MIP adsorbate becomes stronger, reducing the binding
199 affinity and decreasing the adsorption capacity [28,29,35,38].

Langmuir and Freundlich models have been used to describe the binding characteristics of the MIP adsorbents prepared for PFAS extraction. The Langmuir model assumes that binding sites present on the adsorbent surface are identical and that adsorption is mainly monolayer, whereas the Freundlich model assumes binding sites are different and adsorption is multilayer on a heterogeneous surface. The adsorption isotherms of several PFAS MIPs revealed that the Langmuir model describes the adsorption behavior of PFAS on reported MIPs adsorbents well [28,29,35,36,38], while for others the Freundlich model seems to provide a better fit to the experimental results [34,39,40] (Table 2).

Since the knowledge of the adsorption kinetics between analyte and adsorbent is an important feature for extraction applications, it has been studied by most authors who prepared MIPs for PFAS. The two kinetics models used for describing PFASs binding are: the pseudo-second-order kinetics model and the pseudo-first-order kinetics model. In almost all MIPs for PFAS, the pseudo-second-order kinetics model fits the experimental data better than the pseudo-first-order model. This indicates that the PFAS adsorption by the MIPs follows chemical reaction mechanisms, such as electrostatic interactions reported between the selected PFAS and MIP [30,38] , in addition to hydrogen bonding and hydrophobic interactions in some cases [27,36]. The results of adsorption kinetics studies of MIPs adsorbents for PFAS show that the time to reach adsorption equilibrium ranges between 25 min [25] to 80 h [34]. This recorded time seems reasonable compared to other types of adsorbents where similar or more prolonged time was required in some reports. For example, GAC adsorbents required between 3 and 240 h to reach equilibrium [43,44], PAC adsorbents reported equilibrium time between 1h and 24 h [45,46], resins adsorbents reached equilibrium after 2 to 168 h [44,47] and mineral adsorbents like clays reached equilibrium only after 0.3 h [48]. After the sorption experiments, several synthesized MIPs were regenerated completely and re-used at least in five consecutive adsorption-regeneration cycles without losing adsorption capacity for PFAS [35]. The MIP adsorbents showed excellent mechanical stability and their practical applicability in direct removal from real water samples was demonstrated.

2.3. Performances of the adsorbents

The establishment of adsorption isotherms commonly allows the determination of the binding capacity of sorbents. Several factors influence the binding capacity such as the physicochemical characteristics of the sorbent (specific surface area, pore distribution, particle size), the solution temperature and pH and the PFASs concentration. The binding capacity of MIPs for PFASs varies significantly, ranging from 1.289 [37] to 1455.5 $mg \cdot g^{-1}$ [30] for PFOS and from 5.45 to 12.4 $mg \cdot g^{-1}$ for PFOA as detailed in Table 2.

An important aspect of an adsorbent performance is its selectivity toward the target in a real media because of the complexity of the matrix and the usually low concentration of the target in such medium. Improving the selectivity will increase the performances of the adsorbent. The advantages of MIPs over other adsorbents are expected to be their high affinity as well as their high specificity toward the target molecule so they can isolate the target analyte from interfering species in a sample. The specific recognition process of the MIPs adsorbent towards the template mainly depends on the adsorbent characteristics, e.g. the imprinted cavities possessing distinct size and shape matching the targets and the specific functional groups involving diverse interactions between the target and the MIP. Unlike traditional adsorbents and NIPs, MIPs benefit

from the presence of specific imprinted sites which can selectively extract targets from complex real samples.

In a first step, the imprinting effect which is an indicator of the presence of specific binding cavities in the MIP can be evaluated by comparing the binding capacity of the MIP with that of the corresponding NIP and estimating the imprinting factor as the ratio of these two values. By doing so, as presented in table 2, it appears that the PFAS binding capacity of MIPs goes from 1.01 [29] up to 4.95 [32]-fold higher than that of the corresponding NIP in presence of the pure target. For instance, as shown in the Figure 4.a, maximum PFOS binding capacity of MIP-CMSs (75.99 $mg.g^{-1}$) was almost two times that of NIP-CMSs (43.94 $mg.g^{-1}$), indicating the specific binding property of the MIP-CMSs [38]. The studies of Cao and co-workers enable a comparison between conventional AAM-based MIPs adsorbents prepared by precipitation polymerization [28] and surface-imprinted MWCNTs-MIPs adsorbents [35] both prepared under comparable conditions. MWCNTs-MIPs had an adsorption capacity toward PFOA 2.3-fold greater than the conventional MIP. Moreover, the time to reach adsorption equilibrium for these MWCNTs-MIPs appears to be 8-fold lower than in the case of the corresponding conventional AAM-based MIPs. In addition, the maximum adsorption capacity of MWCNTs-MIPs (12.4 $mg.g^{-1}$) was almost two times that of MWCNTs-NIPs (7.44 $mg.g^{-1}$), whereas, AAM-MIPs and AAM-NIPs have similar binding capacities with a imprinting factor of only 1.08. This comparison clearly highlights the advantages of the surface imprinting technique. In the surface imprinting method, the binding sites are accessible at the particles surface, which makes rebinding and removal of target molecule in the polymer network quicker and easier.

Comparing the adsorption capacities toward PFASs of MIP adsorbents with those of clay minerals shows that the performances of MIPs are higher: clay minerals showed adsorption capacities ranging from 0.29 to 0.31 $mg{\cdot}g^{-1}$ for PFOS and 0.10 to 0.11 $mg{\cdot}g^{-1}$ for PFOA [48]. However, MIPs binding capacities are lower than those of other traditional adsorbents such as activated carbon or classical polymeric resins. For instance, the reported adsorption capacity of GAC ranges from 71.6 to 290 $mg{\cdot}g^{-1}$ for PFOS and 41.3 – 120 $mg{\cdot}g^{-1}$ for PFOA while the PAC has an adsorption capacity around 560 $mg{\cdot}g^{-1}$ for PFOS and 290-500 $mg{\cdot}g^{-1}$ for PFOA, whereas, resins showed adsorption capacities ranging between 200 to 2390 $mg{\cdot}g^{-1}$ for PFOS and 525-1500 $mg{\cdot}g^{-1}$ for PFOA [26]. All these traditional sorbents usually suffer from a lack of selectivity towards the targets; then other matrix components are co-extracted with target analytes. Only a limited number of papers demonstrated the selectivity of traditional adsorbents to the class of PFAS compounds [49–51]. The major limitation of these adsorbents is their lack of their selective ability toward one single target PFAS from other PFAS molecules. From this perspective, MIPs appear to be a good choice to improve the selectivity of the extraction process to one PFAS analyte from interferents.

The specificity of the MIPs is evaluated in presence of interferents in binary or multi-component competitive solutions. Comparison of the removal rates of MIPs and NIPs for the template with respect to the interferents shows that MIPs have higher specific binding preference toward the template against interferents compared to NIPs. For several synthesized MIPs adsorbents for PFAS, it was found that other contaminants with different molecular size, structures, functional groups and polarities such as phenol, 2,4-dichlorophenoxy acetic acid [34,35], bisphenol A and dibutyl phthalate [40], sodium dodecylsulfate and sodium dodecylbenzene-sulfonate [38] had little influence on the adsorption of the target. Moreover, when

other PFAS competitive pollutants having similar molecular structures were tested, the MIP adsorbents showed significantly better selectivity toward the template compared to other PFAS interferents in single and mixture solutions. However, the competitive PFAS with longer chains could also be adsorbed onto the MIPs adsorbents in competition with shorter chain analogues [28,29,35]. For example, it was observed that MIPs prepared for PFOA (8 carbons) showed higher adsorption rate towards long-chain PFASs such as PFOS (8 carbons), PFNA (9 carbons), PFDA (10 carbons), PFUnA (11 carbons), PFDoA (12 carbons) than short-chains PFASs like PFBS and PFBA (4 carbons), PFPeA (5 carbons), PFHxS and PFHxA (6 carbons), PFHpA (7 carbons) (Figure 4.b). This might be due to the strong hydrophobicity of long-chain PFASs.

The practical applicability of MIP adsorbents in enrichment and separation was demonstrated by performing direct removal of PFAS from real samples such as tap, lake and river water samples, as well as human serum, pork or milk samples. The impurities in real environment can often interfere with the binding of the analyte and decreases the adsorption efficiency. In real water samples spiked with 5 μM PFOS, the removal rate of MMIPs and MSNs/MIPs toward PFOS were in the range of 53.06-55.66% [36]and 61.68-76.12% [34] respectively. Excellent recovery rates (77.0-96.4%) were obtained within human serum and water samples spiked in the concentration range between 5 and 200 $ng.L^{-1}$ [37]. In another example, the MWCNTs-MIPs showed better recognition ability toward PFOA (removal rate of 74.3%) compared to corresponding NIPs (removal rate of 38.1%) in tap water spiked with 100 $\mu g.L^{-1}$ PFOA in a mixture with other competitive PFAS[35]. For the detection of trace levels of long-chain PFAS in pork sample and in milk, molecularly imprinted phenolic resins were used[31,32]. In pork sample, PFOA was not detected in any of the prepared samples, PFNA was detected in six samples in the concentration range of 5.21–19.04 $ng.g^{-1}$, and PFDA was detected in three samples in the concentration range of 0.13–0.72 $ng.g^{-1}$. Whereas in milk sample, trace PFOA was detected in fifteen milk samples at concentrations of 0.12–2.19 $ng.mL^{-1}$, and PFOS was detected in four milk samples at concentrations of 0.08–0.31 $ng.mL^{-1}$. These results confirm that molecularly imprinted polymers are selective and accurate for determining trace levels of PFASs in complicated real samples.

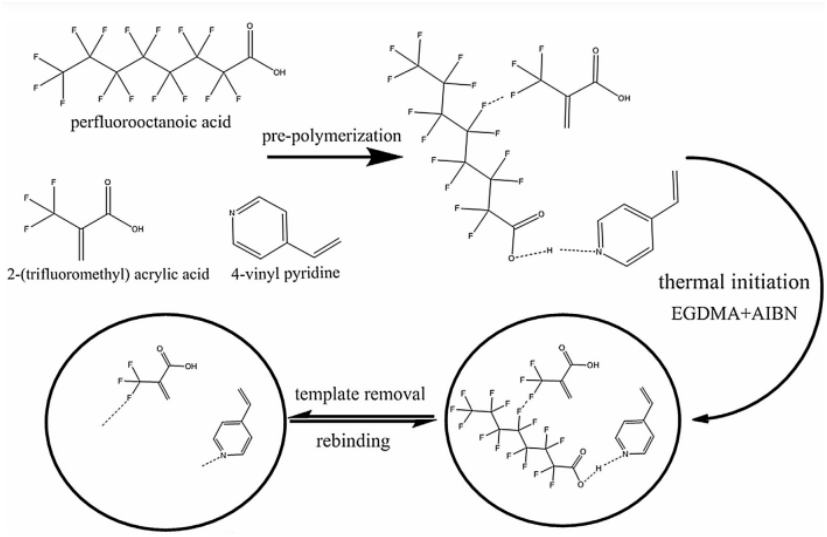

Fig. 2. *Synthesis scheme of a binary functional monomer MIP based on TFMMA and 4-VPy (Reprinted with permission from Elsevier, Copyright 2017 [29]).*

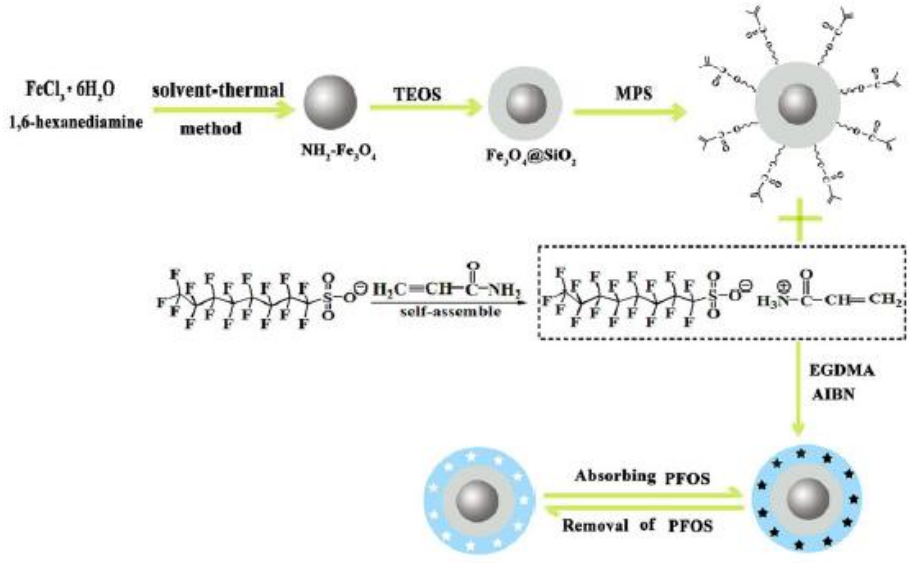

Fig. 3. *Preparation process of MMIPs for PFOS (Reprinted with permission from John Wiley and Sons, Copyright 2017 [36]).*

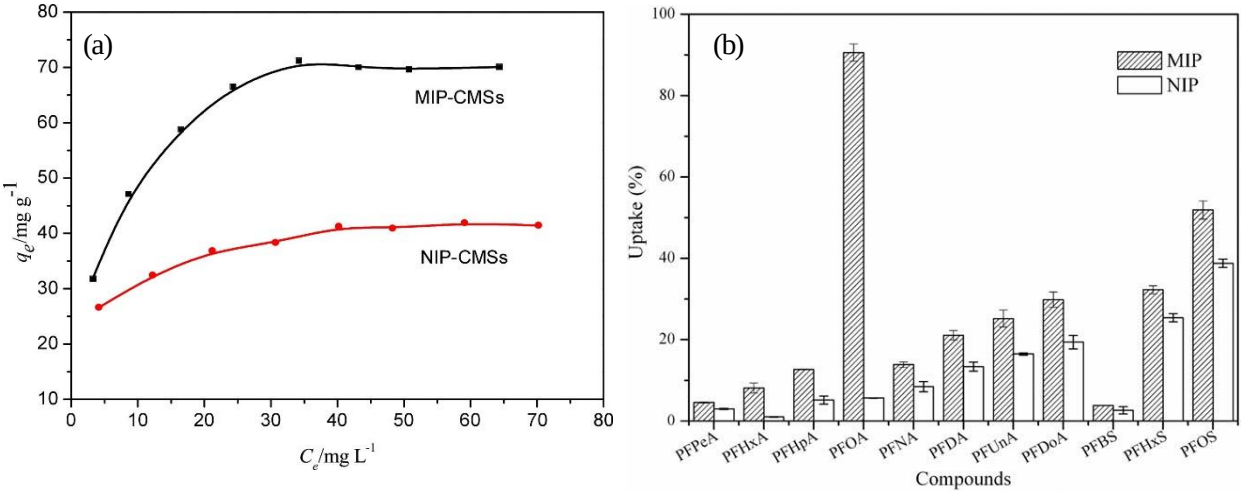

Fig. 4. (a) *Adsorption isotherm of PFOS on MIP-CMSs and NIP-CMSs (Reprinted with permission from Science Direct, Copyright 2018 [38]).* ***(b)*** *Comparison of the adsorption capacity of PFOA with other PFASs on the MIP and NIPs adsorbents (Reprinted with permission from John Wiley and Sons, Copyright 2016[35]).*

Table 2. *Summary of PFAS absorption methods using MIPs,* [a] *Maximum adsorption capacity of MIP,* [b] *Maximum adsorption capacity of NIP,* [c] *Calculated imprinting factor (IF) =* $\frac{Q_{e-MIP}}{Q_{e-NIP}}$

Template	Monomer	Crosslinker	Polymerization method	$Q_{e\text{-}MIP}$[a] ($mg.g^{-1}$)	$Q_{e\text{-}NIP}$[b] ($mg.g^{-1}$)	Imprinting factor[c]	Interferents	Reusability	Real samples	Mode of use	Ref
PFOS	-	ECH	Cross-linking of chitosan	1455.52	1203.51	1.21	PFOA, 2,4-D, SDBS, PCP, phenol	5 cycles	-	Dispersive mode	[30]
PFOS or PFOA	4-VPy	EGDMA or TRIA	Bulk polymerization	-	-		2,4-D	-	-	Dispersive mode	[27]
PFOA	AAM	EGDMA	Precipitation polymerization	5.45	5.04	1.08	PFPeA, PFHxA, PFHpA, PFNA, PFDA, PFUnA, PFDoA, PFBS, PFHxS, PFOS	5 cycles		Dispersive mode	[28]
PFOA	4-Vpy and TFMAA	EGDMA	Precipitation polymerization	6.42 for PFOA	6.31 for PFOA	1.01	PFPA, PFHxA, PFOA, PFNA, PFDA, PFUnA, PFDoA, PFOS, PFBS, PFHxS	5 cycles	Spiked lake water (1 $mg.L^{-1}$)	Dispersive mode	[29]
				6.27 for PFOS	5.31 for PFOS	1.18					
PFOS	AAM	EGDMA	Surface imprinting	2.401	1.164	2.06	PFOA, SDS, SDBS	5 cycles	Spiked tap and river water (5 µM)	Dispersive mode	[36]
PFOS	Dopamine		Self-polymerization of dopamine	1.289 for Low affinity binding site 0.556 for high affinity binding site	0.331	1.75	PFOA, SDBS, CTAB, phenol, PFHSK, F-53B	5 cycles	Spiked lake water, river water, human serum (5-200 ng/L)	SPE	[37]

PFOS	APTES	TEOS	Surface imprinting	21.10	9.78	2.15	PFOA, SDS, SDBS	5 cycles	Spiked tap and river water (5 μM)	Dispersive mode	[34]
PFOS	MTAC and TFMAA	MBA	Surface imprinting	75.99	43.94	1.72	PFOA, PFHSB, PFKSB, F53-B, BPA, DBP, NP	4 cycles	-	Dispersive mode	[38]
PFOA	AAM	EGDMA	Surface imprinting	12.4	7.44	1.69	PFPeA, PFHxA, PFHpA, PFNA, PFDA, PFBS, PFHxS, PFOS	5 cycles	Spiked tap water (100 $\mu g.L^{-1}$)	Dispersive mode	[35]
PFOA	AAM	EGDMA	Surface imprinting	0.8125 ($\mu g.cm^{-1}$)		-	PFOS, PFHA, 2,4-D			Dispersive mode	[40]
PFOA	MAA	TRIM	Surface imprinting		-	-	PFBA, PfeA, PFOA, PFHxA, PFHpA			Dispersive mode	[39]
PFTeDA	4-mercaptophenol	Glutaraldehyde	Bulk polymerization				Atraton, Prometryn, Sulfamethoxaazole, β -Estradiol		Pork samples	Dispersive SPE	[31]
PFNA	*m*-aminophenol	Glutaraldehyde	Bulk polymerization	-	-	4.95 for PFOA 3.76 for PFOS	Sulfamethazine, sulfamethoxazole, florfenicol, thiamphenicol		Milk samples	Dispersive filter extraction	[32]

3. MIPs as selective sensing materials for PFAS

In recent years, new sensor technologies have emerged to try to address the challenge of PFAS detection as a more deployable means to monitoring these pollutants. Innovations include colorimetric sensing [52], precursor detection using the total oxidisable precursor assay [53] and MIP-based sensors. The following section summarizes MIP-based sensor materials created for PFAS detection in aqueous environments according to their detection type.

3.1. Electrochemical sensors

Electrochemical transduction plays a big role in diversifying sensors technology for bioanalytical and environmental applications [54,55]. The immobilization of MIPs on the surface of electrodes offers an alternative to biomolecule-based materials, potentially overcoming classical sensing challenges related to biological recognition such as high cost, instability and selectivity [56–59].

To date, only a few publications have been reported for PFAS-specific detection (Table 3). It is interesting to note that all the strategies reported for PFAS sensing rely on soft (non-crosslinked), electroactive polymers, that are often produced using electropolymerisation methods. This approach offers several advantages compared to chemical polymerization methods, namely the use of aqueous solvents, control of the polymer layer characteristics such as thickness, conductivity etc. and good adhesion to the base electrode material [60]. Electrochemical synthesis of MIPs using o-phenylenediamine (oPD) (also known as 1,2-benzenediamine) as a starting material has been reported as a promising approach to MIP synthesis. Indeed the homopolymer of o-phenylenediamine (poly(o-phenylenediamine)) was one of the first examples of electrochemically synthesized MIPs, and was used for the selective detection of glucose [61]. Their polymer films are considered rigid and stable. Poly-oPD (Figure 4) is non-conductive at pH 5.2, making it a good candidate for capacitance-based sensors [62]. oPD is typically electropolymerized via cyclic voltammetry from aqueous solutions on gold or carbon electrodes [63–66] in the presence of PFAS. PFAS is then removed from these films by a wash step (typically water/methanol), and binding of target is monitored indirectly via a bulk redox probe response such as ferrocenecarboxylic acid. Limit of detection (LOD) values as low as 7.5×10^{-3} $\mu g.L^{-1}$ (0.015 nM) for PFOS have been reported using this strategy, falling well below the limit of 0.4 $\mu g.L^{-1}$ set by the WHO [10] for drinking water. It is also noteworthy that this kind of MIP-based sensors can be enhanced by surface modification of the electrode surface with nanomaterials, such as gold nanostars (AuNS) [64]. Selectivity studies [63–65] considered structurally similar interfering analytes to PFOS (some belonging to the PFAS class and others not) and revealed that PFOS-MIP sensors exhibited high affinity towards PFOS compared to non-PFAS interferents, and a lesser selectivity towards PFOS when smaller PFAS interferents were present simultaneously, due to a more favourable competing access to binding sites. Thus, this sensing approach is promising for detecting PFAS in contaminated water, but further enhancement of selectivity remains a challenge to discriminate between the different PFAS, when present in water as a mixture.

The conducting polymer polyaniline (PANI) (Figure 4) has also been used as a soft MIP templating material for several targets [67–70,59],. A paper-based MIP sensor was reported recently for PFOS detection, created through the chemical polymerization of PANI in the presence of PFOS [71]. Aniline

(An)/PFOS was first adsorbed onto the polyester paper substrate, then exposed to oxidant and dopant to create the PFOS encapsulated polymer film. Upon removal of PFOS, the MIP was created whereby, in the presence of PFOS, which is a negative-charge-rich aliphatic acid, PANI conductivity was modulated through PFOS binding. It was proposed that PFOS binding occurred through the electron holes on the nitrogen atoms of aniline, reducing the number of charge carriers on the surface in the film, reducing film conductivity. This sensor had a reported LOD of 1.02 nM, and resistivity tests before and after exposure to spiked water samples showed significant selectivity towards PFOS compared to other PFAS .

Table 3. *Summary of MIP-based PFAS sensing approaches, highlighting the sensor type, monomer and crosslinking materials, polymerization method, substrate, target PFAS, detection method, limit of detection (LoD), linear dynamic range, spiked water samples tested and recovery*

Sensor type	Monomer	Crosslinker	Polymerization method	Substrate	Target molecule	Detection method	LoD ($\mu g.L^{-1}$)	Linear dynamic range ($\mu g.L^{-1}$)	Spiked water sample	Recovery rate	Ref
Electrochemical	oPD	–	Electropolymerization	GCE	PFOS	Voltammetry	0.025	0 – 0.025	–	–	[63]
	oPD	–	Electropolymerization	GCE	PFOS	Voltammetry	7.5×10^{-3}	0.025 – 2.5	Deionised, tap	86 – 93 %	[64]
	oPD	–	Electropolymerization	Au disc electrode	PFOS	Voltammetry	0.02	0.05 – 2.45 and 4.75 – 750	Distilled, tap, bottled	82 - 110 %	[65]
	oPD	–	Electropolymerization	Au-SPE	PFOS	Voltammetry	–	–	–	–	[66]
	An	–	Radical polymerization	Polyester substrate	PFOS	Resistivity	1.02×10^{-3}	$10^{-3} – 10^{-2}$	–	–	[71]
	Py	–	Electropolymerization	Graphite electrode	PFOA	Potentiometry	41.407	$4.14\times 10^{3} – 4.14$	–	–	[72]

Photoelectrochemical	Aam	EGDMA	Photopolymerization	FTO glass	PFOA	Photocurrent response	0.01	0.02 – 1000	Tap, river	98 – 102 %	[73]
	Aam	EGDMA	Photopolymerization	C-SPE	PFOSF	Photocurrent response	0.01	0.05 – 500	Tap, river, lake	92 – 100 %	[74]
	Aam	EGDMA	Photopolymerization	TiO_2 NTAs	PFOS	Photocurrent response	86	250 – 5000	Tap, river, mountain	95 – 117 %	[75]
Electrochemiluminescent	Py	–	Electropolymerization	GCE	PFOA	Electrochemiluminescence	0.01	0.02 – 40 and 50 – 400	Tap, river, lake	96.9 - 103.8%.	[76]
Photoluminescent	APTS	–	Anchoring APTS-FITC conjugates with/without PFOS at surface of SiO2 NPs	SiO_2 NPs	PFOS	Fluorescence	5.57	5.57 – 48.54	Tap, river	95.7 – 101 %	[77]
	Chitosan	ECH	Hydrothermal sol-gel polymerization	Chitosan hydrogel	PFOS	Fluorescence	4×10^{-7}	$2 \times 10^{-5} – 2 \times 10^{-4}$	Serum, urine	81 – 98 %	[78]
	APTES	TEOS	Sol-gel polymerization	Silica shell	PFOA	Photoluminescence	10.35	1.03×10^{2} – 6.2×10^{3}	–	91 -107 %	[79]
Surface plasmon resonance	VBT and PFDA	EGDMA	Thermal polymerization	POF	PFOA	Surface plasmon resonance	0.13	–	–	–	[80]

Polypyrrole (Ppy) (Figure 4) is another widely used conducting polymer in sensing applications [62]. A potentiometric sensor based on Ppy electrodeposited on pencil lead in the presence of PFOA as template was developed to detect fluoro-surfactants from aqueous firefighting foams [72]. Methylene blue was incorporated into the Ppy matrix during electropolymerisation to increase selectivity (forming ion pairs with the anionic surfactants of interest that were only sparingly soluble in water). The PFOA-specific MIPs showed good selectivity towards PFOA compared to 6:2 fluorotelomer sulfonate (6:2 FTS) and PFOS (which has a larger hydrophilic moiety of the sulfonic acid than the carboxylic acid in PFOA). It also showed an interesting response towards SDS and sodium dodecylbenzenesulfonate (SDBS) (both common detergents), which falls outside the scope of this review. However, the SDS-MIP showed no discernible response for smaller interferent molecules, i.e. PFOA, PFOS, 6:2FTS and SDBS, because SDS leaves a larger cavity after its removal, allowing the smaller interferents to bind to the MIP cavities. Thus, the sensor showed great potential as an accessible pre-screening tool for detecting anionic surfactants. However, efforts to test it in water samples instead of aqueous or buffered solutions remain crucial to validate its efficiency.

3.2. Photoelectrochemical sensors

Photoelectrochemical (PEC) sensors have evolved from electrochemistry and exploit the effect of light on photoactive materials to drive photo-induced chemical events associated with charge separation and transfer [81,82]. PFAS has been the target for several MIP-based PEC sensing approaches [73,83,74,75]. The MIP material is based on photopolymerized AAM crosslinked with EGDMA using azobisisobutyronitrile as initiator. In one publication reporting a PEC sensor targeting PFOS, the photoactive material consisted of a highly ordered, vertically aligned TiO_2 NTA serving as a graft polymerization substrate for the Aam-based MIPs [75]. Evaluating the relative change in photocurrent response to PFOS against that of PFAS analogues and non-fluorinated interferents indicated high binding selectivity for PFOS, even when interferent concentration was 20 times greater than PFOS. Sensor repeatability was 2.8 % standard deviation for 10 measurements, and long-term stability after 1 month storage (< 4 % decrease in response) and 3 months storage (<5.1 %). The LOD of this sensor was estimated at 86 $\mu g.L^{-1}$.

In another PEC-based PFAS sensor, an AgI nanoparticle and BiOI nanoflake array (AgI-BiOINFs) immobilised on fluorine-doped tin oxide (FTO) was used as a photoactive electrode and was realised via a successive ionic layer adsorption and reaction method [73]. The array was subsequently grafted with a PFOA MIP. The LOD for PFOA was estimated at 0.01 $\mu g.L^{-1}$, comparable to that achievable with LC-MS/MS. Selectivity towards PFOA was remarkable as the relative change in the photocurrent response of samples containing selected structurally similar non-fluorinated compounds and other PFOA analogues was negligible compared to PFOA-spiked samples. Furthermore, in the presence of interferent compounds, the response to PFOA was not impacted and the superior selectivity for PFOA was attributed to the selective shape and hydrogen bond identification. The recovery rate for spiked tap and river water samples was reported to be in the range of 98.2-102.4 %. The same group later proposed a disposable PEC sensor for PFOSF using a screen-printed carbon electrode functionalised with electrodeposited BiOINF [74] (Figure 5). This surface was then used for grafting the MIP. This method was simpler to realize and offered high selectivity to PFOSF with a 0.01 $\mu g.L^{-1}$ LOD, much lower than the 0.5 $\mu g.L^{-1}$ reported by LC-MS.

3.3. Electrochemiluminescent sensors

The basic principle of electrochemiluminescence (ECL) is that an electrochemically initiated reaction produces molecules at excited states that undergo subsequent relaxation and generate a luminescence emission [84,85]. The smart combination of electrochemistry and chemiluminescence gives ECL several advantages, mainly in avoiding background noise and issues associated with light scattering as it does not require an external light source [85]. Much like PEC sensors, ECL detection using MIPs as selective materials has received considerable attention as an analytical tool for clinical detection of analytes like deoxyribonucleic acid [86], cancer biomarkers [87], bacteria [88] and antibodies [89]. However, reports on MIP-based ECL sensors for PFAS targets in environmental waters are still scarce [90]. One recent example was based on MIP-modified ultrathin graphitic carbon nitride nanosheets (utg-C_3N_4) for the detection of PFOA [76]. The method consisted of modifying a glassy carbon electrode (GCE) with a utg-C_3N_4 dispersion using drop-casting and subsequently carrying out an electropolymerisation of 5 mM pyrrole and 1 mM PFOA via cyclic voltammetry at pH 6. The ECL signal intensity was shown to decrease with increased concentrations of PFOA in a linear fashion over two concentration ranges: 0.02 to 40 $ng.ml^{-1}$ and 50-400 $ng.ml^{-1}$. The LOD was estimated to be 0.01 $ng.ml^{-1}$, significantly lower than those reported using chromatographic methods (25 $ng.L^{-1}$ by LC-MS/MS, for example [91]). The selectivity of the ECL sensor was evaluated, and it was found that the change in ECL intensity was negligible for interfering compounds with similar size and structure to PFOA. Recovery rates in samples of spiked tap, river and lake water were found between 96.9 and 103.8%. The reproducibility and stability of the sensors were investigated, and the RSD was found to be 4.10%.

3.4. Photoluminescent sensors

Fluorescence-based detection methods have received considerable attention thanks to their remarkable sensitivity and versatility in terms of transduction schemes [92,93]. Fluorescent sensors have utilized quantum dots (QDs) [94], nanomaterials [95], conjugated polymers [93] and photoluminescent MIPs (PLMIPs) [96]. There are numerous ways to synthesize PLMIPs, most of which involve copolymerization of fluorescent monomers, or encapsulation with fluorophores or nanomaterials [96]. For instance, a selective detection method for PFOS in water through MIP-capped silica nanoparticles was published [77]. Fluorescein 6-isothiocyanate (FITC) dye was covalently linked to the surface of silica nanoparticles (SiO_2-NPs). Upon binding of PFOS to NH_2 ligands within the specific recognition site, the PFOS-amine complexes formed strongly suppressed the fluorescence emission of the FITC through a charge-transfer mechanism from FITC to PFOS. The LOD was determined to be 5.57 $\mu g.L^{-1}$. Analysis of tap and river water spiked with PFOS revealed a recovery rate from 95.7 to 101%. For samples containing a mixture of PFOS and interfering molecules (PFOA, PFHxA, PFHxS, Phenol, SDBS), the quantitative recovery of PFOS ranged from 97.9 to 106%. Another similar approach for detecting PFOS was developed using a MIP-based fluorescent hydrogel comprising carbon quantum dot (CQD)-doped chitosan [78]. However, it seemed that both the MIP- and NIP-coated CQDs showed fluorescence responses to PFOS, which indicated that the NH_2 groups present at the surface of the MIP- and NIP-coated NPs could also act as binding sites for PFOS through hydrogen bonding and electrostatic interactions. Despite this, as shown through the

imprinting factor (IF) ($K_{SV, MIP}/K_{SV, NIP}$), the specific binding cavities in the MIP hydrogel had stronger adsorption of PFOS and showed higher fluorescence intensities where IF value for analogue molecules ranged from 0.51 to 1.33, compared to 2.75 for PFOS. Cadmium-telluride (CdTe)/cadmium-sulphide (CdS)-based QDs coated with thioglycolic acid (TGA), imprinted with 3-aminopropyltriethoxysilane (APTES) in the presence of PFOA have been reported via sol-gel polymerization [79]. The PL intensity of the MIP-capped QDs decreased by 44% with PFOA bound to the recognition sites compared to the NIP-capped QDs. However, this PL intensity soars to 81.25% after the removal of PFOA, thus confirming the capacity to which PFOA can quench the MIP-capped CdTe/CdS QDs. The PFOA-induced PL quenching was significantly higher than those resulting from analogues using the MIP-capped QDs, however the response was nearly identical using the NIP-capped QDs for these same analogues. Analysis of real water samples showed average recovery rates of PFOA ranging between 91-107% with RSD below 5.6%.

Overall, these PL sensors showed value in coupling selective recognition of MIPs and analyte-dependent emission of various fluorophores such as QDs and fluorescent dyes, which allows for more applications in the optical detection of PFAS in real water samples.

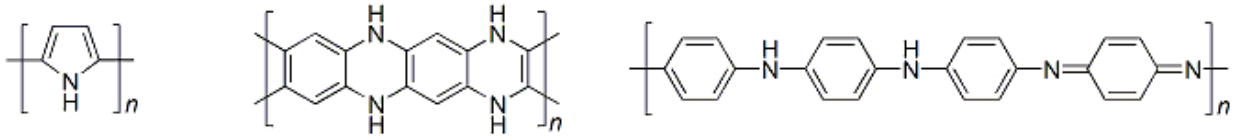

polypyrrole (PPy)

poly-ortho-phenylenediamine (Poly-*o*PD)
(benzenoid unit)

polyaniline (PANI)
(emeraldine base)

Fig. 4 *Chemical structures of (a) Ppy, (b) Poly-oPD, and (c) PANI*

Fig. 5. *Schematic of photoelectrochemical detection of PFOSF using a MIP based BiOINFs on SPE sensing strip (Reprinted with permission from Elsevier, Copyright 2018* [74]*).*

3.5. Surface plasmon resonance (and optical intensity-based sensors)

One of the relatively new optical detection methods is plasmon surface resonance (SPR). Popularized in the 90s by biosensor companies [97], this refractive index-based technique allows the determination of the kinetic parameters of molecular interactions. However, it can also be used for real-time, label-free analysis of analytes in complex matrices with superior sensitivity [97,98]. The integration of MIPs to SPR sensors was very favorable and shifted research to achieve more sensitive detection. However, most of this research is geared toward detecting complex biomolecules and biomolecular assays, such as proteins [98,99], antigens [100], and antibiotics [101]. There are very few studies done to detect pollutants and non-biological analytes using SPR and MIPs, namely explosives [102], pesticides [103,104], and PFAS. The latter received attention with the recent development of a MIP based plasmonic plastic optical fiber (POF) sensor to detect PFOA in water [80]. In this method, the optical platform consists of a POF (poly(methyl methacrylate)) topped with an optical (photoresist) buffer layer (1.5 μm) and finished off with a sputtered thin gold film (60 nm in thickness). The photoresist optical layer enhances the sensor's performance by offering a higher refractive index than the POF core in the desired visible range. On the other hand, the gold film provides a support to the MIP receptor layer, whereby it can be directly deposited (in-situ polymerization) without any prior surface modification, which is a key advantage for this kind of sensors. Thus, the binding of the target analyte to the recognition site in the MIP layer causes a change in the refractive index between this layer and the gold film, which causes a shift in the resonance wavelength (which can be quantified through SPR spectroscopy). However, when PFOA was present in the bulk solution, the change in resonance wavelength (and refractive index) recorded was a decrease rather than the usual increase. The success of this sensor was confirmed by binding and non-binding experiments, where the signal recorded with the SPR-POF-NIP showed no shift of the resonance wavelength, whereas the SPR-POF-MIP showed a clear shift into smaller values (decrease in refractive index), with an LoD of 0.13 $\mu g.L^{-1}$, comparable with that of an SPR-POF platform with a bio-receptor (antibody) of 0.24 $\mu g.L^{-1}$, previously developed by the same research team for the detection of PFOA [105].

This SPR-POF-MIP sensor also showed similar responses when adding PFAS compounds with varying carbon chain lengths (C4-C11), compared to PFOA alone in the sample solutions, with a slight difference in resonance wavelength variation that can be explained with the change in refractive index in the MIP layer due to the change in molecular size of the binding analyte present.

In a similar study done by the same group [106], an intensity-based POF sensor paired with a MIP receptor was used for the first time to detect C4 to C12 PFAS in water samples. This POF-MIP sensor is virtually identical to the SPR-POF-MIP discussed previously [80], except for the gold film and optical buffer layer (which provide the SPR properties) and the spin-coated MIP layer on the POF platform. This type of detection showed promise for PFAS detection in water samples, offering a lower cost of preparation and experimental set-up, convenience to use under environmental conditions and good repeatability.

4. Conclusions

PFAS are emerging as chemicals of concern because of the reported risks to human health, notably their capacity to act as endocrine disruptors, and their environmental safety as they are persistent and

bioaccumulative. PFOA and PFOS are of particular interest as they are very widely used in the manufacture of household objects, cleaning supplies and as firefighting foams.

MIPs are popular as selective recognition elements due to their unique ability to bind specific targets with high affinity. As traditional adsorption materials for PFAS, such as activated carbon, biomaterials and mineral materials, lack in selectivity, MIPs were introduced as an alternative for more efficient enrichment methods of PFAS. The methods of MIP preparation range from traditional polymerization techniques such as bulk and precipitation polymerization, to more innovative ones like surface imprinting techniques involving functionalized nanomaterials (such as MWCNTs and CMSs). Many of the PFAS-MIP sensors reviewed here exhibit higher affinity towards PFAS than for competing minerals present in sample matrix - river, lake, sea water. Lab testing is performed on collected water samples typically and on-site testing is less common. However, when the field moves onto this, no doubt more challenges will arise. High selectivity towards PFAS is particularly evident when in competition with structurally related non-PFAS. As for competing PFAS pollutants, long-chained molecules are more likely to bind to PFAS-MIPs than to their short-chained analogues. Moreover, regeneration studies on some PFAS-MIPs do demonstrate reusability with conserved adsorption capacity and mechanical stability, further highlighting the advantages of using MIPs as selective sorbents. The reported detection methods used included electrochemical, photoluminescent, photoelectrochemical, electrochemiluminescent, and surface plasmon-based strategies. This versatility is a further advantage as it provides alternatives for industrial scale sensor manufacture. Finally, it is important to stress that while MIP-based sensors will never replace traditional, more established detection techniques, PFAS-MIP sensors inherently present advantages in terms of portability, miniaturisation and cost-effectiveness. Although sensor technology is always more challenged in terms of analytical sensitivity, there are some reports emerging of PFAS-MIP sensors with sensitivities reaching ppb and even ppt levels, targets that must be delivered upon to comply with PFAS regulations.

Acknowledgements

This work was financially supported by NEMO ERANET MarTERA research program, funded by the ANR (ANR-20-MART-0001) and the Marine Institute.

References

[1] N. Ding, S.D. Harlow, J.F. Randolph Jr, R. Loch-Caruso, S.K. Park, Perfluoroalkyl and polyfluoroalkyl substances (PFAS) and their effects on the ovary, Hum. Reprod. Update. 26 (2020) 724–752. https://doi.org/10.1093/humupd/dmaa018.

[2] E. Gagliano, M. Sgroi, P.P. Falciglia, F.G.A. Vagliasindi, P. Roccaro, Removal of poly- and perfluoroalkyl substances (PFAS) from water by adsorption: Role of PFAS chain length, effect of organic matter and challenges in adsorbent regeneration, Water Res. 171 (2020) 115381-115411. https://doi.org/10.1016/j.watres.2019.115381.

[3] R.C. Buck, J. Franklin, U. Berger, J.M. Conder, I.T. Cousins, P. de Voogt, A.A. Jensen, K. Kannan, S.A. Mabury, S.P. van Leeuwen, Perfluoroalkyl and polyfluoroalkyl substances in the environment: Terminology, classification, and origins, Integr. Environ. Assess. Manag. 7 (2011) 513–541. https://doi.org/10.1002/ieam.258.

[4] P. Zareitalabad, J. Siemens, M. Hamer, W. Amelung, Perfluorooctanoic acid (PFOA) and perfluorooctanesulfonic acid (PFOS) in surface waters, sediments, soils and wastewater – A review on

concentrations and distribution coefficients, Chemosphere. 91 (2013) 725–732. https://doi.org/10.1016/j.chemosphere.2013.02.024.
[5] W. Völkel, O. Genzel-Boroviczény, H. Demmelmair, C. Gebauer, B. Koletzko, D. Twardella, U. Raab, H. Fromme, Perfluorooctane sulphonate (PFOS) and perfluorooctanoic acid (PFOA) in human breast milk: Results of a pilot study, Int. J. Hyg. Environ. Health. 211 (2008) 440–446. https://doi.org/10.1016/j.ijheh.2007.07.024.
[6] B.D. Key, R.D. Howell, C.S. Criddle, Defluorination of Organofluorine Sulfur Compounds by *Pseudomonas* Sp. Strain D2, Environ. Sci. Technol. 32 (1998) 2283–2287. https://doi.org/10.1021/es9800129.
[7] H.Fr. Schröder, R.J.W. Meesters, Stability of fluorinated surfactants in advanced oxidation processes—A follow up of degradation products using flow injection–mass spectrometry, liquid chromatography–mass spectrometry and liquid chromatography–multiple stage mass spectrometry, J. Chromatogr. A. 1082 (2005) 110–119. https://doi.org/10.1016/j.chroma.2005.02.070.
[8] Directive 2013/39/EU of the European Parliament and of the Council of 12 August 2013 amending Directives 2000/60/EC and 2008/105/EC as regards priority substances in the field of water policyText with EEA relevance, (n.d.) 17.
[9] Envionmental Protection Agency (EPA), Provisional Health Advisories for Perfluorooctanoric acid (PFOA) and Perfluorooctane Sulfonate (PFOS), (n.d.). http:// water.epa.gov/action/advisories/drinking/upload/2009_01_15_criteria_drinking_ pha_PFOA_PFOS.PDF.
[10] Europen Commission, Proposal for a DIRECTIVE OF THE EUROPEAN PARLIAMENT AND OF THE COUNCIL on the quality of water intended for human consumption (recast), (2018).
[11] D.M. Lemal, Perspective on Fluorocarbon Chemistry, J. Org. Chem. 69 (2004) 1–11. https://doi.org/10.1021/jo0302556.
[12] J.C. Biffinger, H.W. Kim, S.G. DiMagno, The Polar Hydrophobicity of Fluorinated Compounds, ChemBioChem. 5 (2004) 622–627. https://doi.org/10.1002/cbic.200300910.
[13] K.H. Kucharzyk, R. Darlington, M. Benotti, R. Deeb, E. Hawley, Novel treatment technologies for PFAS compounds: A critical review, J. Environ. Manage. 204 (2017) 757–764. https://doi.org/10.1016/j.jenvman.2017.08.016.
[14] A.F. Ojo, C. Peng, J.C. Ng, Assessing the human health risks of per- and polyfluoroalkyl substances: A need for greater focus on their interactions as mixtures, J. Hazard. Mater. 407 (2021) 124863-124876. https://doi.org/10.1016/j.jhazmat.2020.124863.
[15] N.M. Crawford, S.E. Fenton, M. Strynar, E.P. Hines, D.A. Pritchard, A.Z. Steiner, Effects of perfluorinated chemicals on thyroid function, markers of ovarian reserve, and natural fertility, Reprod. Toxicol. 69 (2017) 53–59. https://doi.org/10.1016/j.reprotox.2017.01.006.
[16] K. Haupt, K. Mosbach, Molecularly Imprinted Polymers and Their Use in Biomimetic Sensors, Chem. Rev. 100 (2000) 2495–2504. https://doi.org/10.1021/cr990099w.
[17] K. Karim, F. Breton, R. Rouillon, E.V. Piletska, A. Guerreiro, I. Chianella, S.A. Piletsky, How to find effective functional monomers for effective molecularly imprinted polymers?, Adv. Drug Deliv. Rev. 57 (2005) 1795–1808. https://doi.org/10.1016/j.addr.2005.07.013.
[18] A. Poma, A.P.F. Turner, S.A. Piletsky, Advances in the manufacture of MIP nanoparticles, Trends Biotechnol. 28 (2010) 629–637. https://doi.org/10.1016/j.tibtech.2010.08.006.
[19] D. Refaat, M.G. Aggour, A.A. Farghali, R. Mahajan, J.G. Wiklander, I.A. Nicholls, S.A. Piletsky, Strategies for Molecular Imprinting and the Evolution of MIP Nanoparticles as Plastic Antibodies—Synthesis and Applications, Int. J. Mol. Sci. 20 (2019) 6304-6324. https://doi.org/10.3390/ijms20246304.
[20] A. Azizi, C.S. Bottaro, A critical review of molecularly imprinted polymers for the analysis of organic pollutants in environmental water samples, J. Chromatogr. A. 1614 (2020) 460603-460637. https://doi.org/10.1016/j.chroma.2019.460603.
[21] O.S. Ahmad, T.S. Bedwell, C. Esen, A. Garcia-Cruz, S.A. Piletsky, Molecularly Imprinted Polymers in Electrochemical and Optical Sensors, Trends Biotechnol. 37 (2019) 294–309. https://doi.org/10.1016/j.tibtech.2018.08.009.
[22] X. Shen, L. Zhu, N. Wang, L. Ye, H. Tang, Molecular imprinting for removing highly toxic organic pollutants, Chem Commun. 48 (2012) 788–798. https://doi.org/10.1039/C2CC14654A.

[23] Y. Fuchs, O. Soppera, K. Haupt, Photopolymerization and photostructuring of molecularly imprinted polymers for sensor applications—A review, Anal. Chim. Acta. 717 (2012) 7–20. https://doi.org/10.1016/j.aca.2011.12.026.
[24] Q. Yu, R. Zhang, S. Deng, J. Huang, G. Yu, Sorption of perfluorooctane sulfonate and perfluorooctanoate on activated carbons and resin: Kinetic and isotherm study, Water Res. 43 (2009) 1150–1158. https://doi.org/10.1016/j.watres.2008.12.001.
[25] Z. Du, S. Deng, Y. Bei, Q. Huang, B. Wang, J. Huang, G. Yu, Adsorption behavior and mechanism of perfluorinated compounds on various adsorbents—A review, J. Hazard. Mater. 274 (2014) 443–454. https://doi.org/10.1016/j.jhazmat.2014.04.038.
[26] D.Q. Zhang, W.L. Zhang, Y.N. Liang, Adsorption of perfluoroalkyl and polyfluoroalkyl substances (PFASs) from aqueous solution - A review, Sci. Total Environ. 694 (2019) 133606-133622. https://doi.org/10.1016/j.scitotenv.2019.133606.
[27] S. Deng, D. Shuai, Q. Yu, J. Huang, G. Yu, Selective sorption of perfluorooctane sulfonate on molecularly imprinted polymer adsorbents, Front. Environ. Sci. Eng. China. 3 (2009) 171–177. https://doi.org/10.1007/s11783-009-0017-4.
[28] F. Cao, L. Wang, X. Ren, H. Sun, Synthesis of a perfluorooctanoic acid molecularly imprinted polymer for the selective removal of perfluorooctanoic acid in an aqueous environment, J. Appl. Polym. Sci. 133 (2016) 43192-43201. https://doi.org/10.1002/app.43192.
[29] F. Cao, L. Wang, Y. Tian, F. Wu, C. Deng, Q. Guo, H. Sun, S. Lu, Synthesis and evaluation of molecularly imprinted polymers with binary functional monomers for the selective removal of perfluorooctanesulfonic acid and perfluorooctanoic acid, J. Chromatogr. A. 1516 (2017) 42–53. https://doi.org/10.1016/j.chroma.2017.08.023.
[30] Q. Yu, S. Deng, G. Yu, Selective removal of perfluorooctane sulfonate from aqueous solution using chitosan-based molecularly imprinted polymer adsorbents, Water Res. 42 (2008) 3089–3097. https://doi.org/10.1016/j.watres.2008.02.024.
[31] D. Zou, P. Li, C. Yang, D. Han, H. Yan, Rapid determination of perfluorinated compounds in pork samples using a molecularly imprinted phenolic resin adsorbent in dispersive solid phase extraction-liquid chromatography tandem mass spectrometry, Anal. Chim. Acta. 1226 (2022) 340271-340279. https://doi.org/10.1016/j.aca.2022.340271.
[32] J. Ren, Y. Lu, Y. Han, F. Qiao, H. Yan, Novel molecularly imprinted phenolic resin–dispersive filter extraction for rapid determination of perfluorooctanoic acid and perfluorooctane sulfonate in milk, Food Chem. 400 (2023) 134062-134069. https://doi.org/10.1016/j.foodchem.2022.134062.
[33] C.J. Tan, Y.W. Tong, Molecularly imprinted beads by surface imprinting, Anal. Bioanal. Chem. 389 (2007) 369–376. https://doi.org/10.1007/s00216-007-1362-4.
[34] L. Du, Z. Cheng, P. Zhu, Q. Chen, Y. Wu, K. Tan, Preparation of mesoporous silica nanoparticles molecularly imprinted polymer for efficient separation and enrichment of perfluorooctane sulfonate, J. Sep. Sci. 41 (2018) 4363–4369. https://doi.org/10.1002/jssc.201800587.
[35] F. Cao, L. Wang, Y. Yao, F. Wu, H. Sun, S. Lu, Synthesis and application of a highly selective molecularly imprinted adsorbent based on multi-walled carbon nanotubes for selective removal of perfluorooctanoic acid, Environ. Sci. Water Res. Technol. 4 (2018) 689–700. https://doi.org/10.1039/C7EW00443E.
[36] L. Du, Y. Wu, X. Zhang, F. Zhang, X. Chen, Z. Cheng, F. Wu, K. Tan, Preparation of magnetic molecularly imprinted polymers for the rapid and selective separation and enrichment of perfluorooctane sulfonate, J. Sep. Sci. 40 (2017) 2819–2826. https://doi.org/10.1002/jssc.201700157.
[37] L. Lin, H. Guo, S. Lin, Y. Chen, L. Yan, E. Zhu, K. Li, Selective extraction of perfluorooctane sulfonate in real samples by superparamagnetic nanospheres coated with a polydopamine-based molecularly imprinted polymer, J. Sep. Sci. 44 (2021) 1015–1025. https://doi.org/10.1002/jssc.202000824.
[38] H. Guo, Y. Liu, W. Ma, L. Yan, K. Li, S. Lin, Surface molecular imprinting on carbon microspheres for fast and selective adsorption of perfluorooctane sulfonate, J. Hazard. Mater. 348 (2018) 29–38. https://doi.org/10.1016/j.jhazmat.2018.01.018.

[39] L. Hu, Y. Li, W. Zhang, Characterization and application of surface-molecular-imprinted-polymer modified TiO2 nanotubes for removal of perfluorinated chemicals, Water Sci. Technol. 74 (2016) 1417–1425. https://doi.org/10.2166/wst.2016.321.
[40] Y. Wu, Y. Li, A. Tian, K. Mao, J. Liu, Selective Removal of Perfluorooctanoic Acid Using Molecularly Imprinted Polymer-Modified TiO_2 Nanotube Arrays, Int. J. Photoenergy. 2016 (2016) 1–10. https://doi.org/10.1155/2016/7368795.
[41] K.-U. Goss, The p K_a Values of PFOA and Other Highly Fluorinated Carboxylic Acids, Environ. Sci. Technol. 42 (2008) 456–458. https://doi.org/10.1021/es702192c.
[42] D. Brooke, A. Footitt, T.A. Nwaogu, Great Britain, Environment Agency, Environmental risk evaluation report ; Perfluorooctanesulphonate (PFOS), Environment Agency, Bristol, 2009.
[43] D. Zhang, Q. He, M. Wang, W. Zhang, Y. Liang, Sorption of perfluoroalkylated substances (PFASs) onto granular activated carbon and biochar, Environ. Technol. 42 (2021) 1798–1809. https://doi.org/10.1080/09593330.2019.1680744.
[44] Y. Zhi, J. Liu, Adsorption of perfluoroalkyl acids by carbonaceous adsorbents: Effect of carbon surface chemistry, Environ. Pollut. 202 (2015) 168–176. https://doi.org/10.1016/j.envpol.2015.03.019.
[45] Y. Qu, C. Zhang, F. Li, X. Bo, G. Liu, Q. Zhou, Equilibrium and kinetics study on the adsorption of perfluorooctanoic acid from aqueous solution onto powdered activated carbon, J. Hazard. Mater. 169 (2009) 146–152. https://doi.org/10.1016/j.jhazmat.2009.03.063.
[46] J. Li, Q. Li, L. Li, L. Xu, Removal of perfluorooctanoic acid from water with economical mesoporous melamine-formaldehyde resin microsphere, Chem. Eng. J. 320 (2017) 501–509. https://doi.org/10.1016/j.cej.2017.03.073.
[47] Y. Gao, S. Deng, Z. Du, K. Liu, G. Yu, Adsorptive removal of emerging polyfluoroalky substances F-53B and PFOS by anion-exchange resin: A comparative study, J. Hazard. Mater. 323 (2017) 550–557. https://doi.org/10.1016/j.jhazmat.2016.04.069.
[48] L. Zhao, J. Bian, Y. Zhang, L. Zhu, Z. Liu, Comparison of the sorption behaviors and mechanisms of perfluorosulfonates and perfluorocarboxylic acids on three kinds of clay minerals, Chemosphere. 114 (2014) 51–58. https://doi.org/10.1016/j.chemosphere.2014.03.098.
[49] M. Mehmandoust, N. Erk, C. Karaman, O. Karaman, An electrochemical molecularly imprinted sensor based on CuBi2O4/rGO@MoS2 nanocomposite and its utilization for highly selective and sensitive for linagliptin assay, Chemosphere. 291 (2022) 132807-132817. https://doi.org/10.1016/j.chemosphere.2021.132807.
[50] Z. Du, S. Deng, S. Zhang, B. Wang, J. Huang, Y. Wang, G. Yu, B. Xing, Selective and High Sorption of Perfluorooctanesulfonate and Perfluorooctanoate by Fluorinated Alkyl Chain Modified Montmorillonite, J. Phys. Chem. C. 120 (2016) 16782–16790. https://doi.org/10.1021/acs.jpcc.6b04757.
[51] Y. Zhou, Z. He, Y. Tao, Y. Xiao, T. Zhou, T. Jing, Y. Zhou, S. Mei, Preparation of a functional silica membrane coated on Fe3O4 nanoparticle for rapid and selective removal of perfluorinated compounds from surface water sample, Chem. Eng. J. 303 (2016) 156–166. https://doi.org/10.1016/j.cej.2016.05.137.
[52] Md. Al Amin, Z. Sobhani, S. Chadalavada, R. Naidu, C. Fang, Smartphone-based / Fluoro-SPE for selective detection of PFAS at ppb level, Environ. Technol. Innov. 18 (2020) 100778-100785. https://doi.org/10.1016/j.eti.2020.100778.
[53] M. Al Amin, Y. Luo, A. Nolan, F. Robinson, J. Niu, S. Warner, Y. Liu, R. Dharmarajan, M. Mallavarapu, R. Naidu, C. Fang, Total oxidisable precursor assay towards selective detection of PFAS in AFFF, 2021.
[54] R.B. Clark, J.E. Dick, Towards deployable electrochemical sensors for per- and polyfluoroalkyl substances (PFAS), Chem. Commun. 57 (2021) 8121–8130. https://doi.org/10.1039/D1CC02641K.
[55] D. Grieshaber, R. MacKenzie, J. Voros, E. Reimhult, Electrochemical Biosensors - Sensor Principles and Architectures, (2008) 59.
[56] B. Mostafiz, S.A. Bigdeli, K. Banan, H. Afsharara, D. Hatamabadi, P. Mousavi, C.M. Hussain, R. Keçili, F. Ghorbani-Bidkorbeh, Molecularly imprinted polymer-carbon paste electrode (MIP-CPE)-based sensors for the sensitive detection of organic and inorganic environmental pollutants: A review, Trends Environ. Anal. Chem. 32 (2021) e00144-e00144. https://doi.org/10.1016/j.teac.2021.e00144.

[57] Y. Pan, D. Shan, L. Ding, X. Yang, K. Xu, H. Huang, J. Wang, H. Ren, Developing a generally applicable electrochemical sensor for detecting macrolides in water with thiophene-based molecularly imprinted polymers, Water Res. 205 (2021) 117670-117678. https://doi.org/10.1016/j.watres.2021.117670.
[58] C. Unger, P.A. Lieberzeit, Molecularly imprinted thin film surfaces in sensing: Chances and challenges, React. Funct. Polym. 161 (2021) 104855-104864. https://doi.org/10.1016/j.reactfunctpolym.2021.104855.
[59] Y. Zhang, Z. Liu, Y. Wang, X. Kuang, H. Ma, Q. Wei, Directly assembled electrochemical sensor by combining self-supported CoN nanoarray platform grown on carbon cloth with molecularly imprinted polymers for the detection of Tylosin, J. Hazard. Mater. 398 (2020) 122778-122786. https://doi.org/10.1016/j.jhazmat.2020.122778.
[60] R. Crapnell, A. Hudson, C. Foster, K. Eersels, B. Grinsven, T. Cleij, C. Banks, M. Peeters, Recent Advances in Electrosynthesized Molecularly Imprinted Polymer Sensing Platforms for Bioanalyte Detection, Sensors. 19 (2019) 1204-1231. https://doi.org/10.3390/s19051204.
[61] C. Malitesta, I. Losito, P.G. Zambonin, Molecularly Imprinted Electrosynthesized Polymers: New Materials for Biomimetic Sensors, Anal. Chem. 71 (1999) 1366–1370. https://doi.org/10.1021/ac980674g.
[62] C. Malitesta, E. Mazzotta, R.A. Picca, A. Poma, I. Chianella, S.A. Piletsky, MIP sensors – the electrochemical approach, Anal. Bioanal. Chem. 402 (2012) 1827–1846. https://doi.org/10.1007/s00216-011-5405-5.
[63] R. Kazemi, E.I. Potts, J.E. Dick, Quantifying Interferent Effects on Molecularly Imprinted Polymer Sensors for Per- and Polyfluoroalkyl Substances (PFAS), Anal. Chem. 92 (2020) 10597–10605. https://doi.org/10.1021/acs.analchem.0c01565.
[64] D. Lu, D.Z. Zhu, H. Gan, Z. Yao, J. Luo, S. Yu, P. Kurup, An ultra-sensitive molecularly imprinted polymer (MIP) and gold nanostars (AuNS) modified voltammetric sensor for facile detection of perfluorooctance sulfonate (PFOS) in drinking water, Sens. Actuators B Chem. 352 (2022) 131055-131065. https://doi.org/10.1016/j.snb.2021.131055.
[65] N. Karimian, A.M. Stortini, L.M. Moretto, C. Costantino, S. Bogialli, P. Ugo, Electrochemosensor for Trace Analysis of Perfluorooctanesulfonate in Water Based on a Molecularly Imprinted Poly(*o* -phenylenediamine) Polymer, ACS Sens. 3 (2018) 1291–1298. https://doi.org/10.1021/acssensors.8b00154.
[66] G. Moro, D. Cristofori, F. Bottari, E. Cattaruzza, K. De Wael, L.M. Moretto, Redesigning an Electrochemical MIP Sensor for PFOS: Practicalities and Pitfalls, Sensors. 19 (2019) 4433-4445. https://doi.org/10.3390/s19204433.
[67] J. Luo, J. Huang, Y. Wu, J. Sun, W. Wei, X. Liu, Synthesis of hydrophilic and conductive molecularly imprinted polyaniline particles for the sensitive and selective protein detection, Biosens. Bioelectron. 94 (2017) 39-46. https://doi.org/10.1016/j.bios.2017.02.035.
[68] A. Kausaite-Minkstimiene, V. Mazeiko, A. Ramanaviciene, A. Ramanavicius, Enzymatically synthesized polyaniline layer for extension of linear detection region of amperometric glucose biosensor, Biosens. Bioelectron. 26 (2010) 790-797. https://doi.org/10.1016/j.bios.2010.06.023.
[69] L. Özcan, M. Sahin, Y. Sahin, Electrochemical Preparation of a Molecularly Imprinted Polypyrrole-modified Pencil Graphite Electrode for Determination of Ascorbic Acid, Sensors (Basel) 8 (2008) 5792-5805. https://doi.org/10.3390/s8095792
[70] A.A. Wani, A. M. Khan, Y. K. Manea, M. A.S. Salem, M. Shahadat, Selective adsorption and ultrafast fluorescent detection of Cr(VI) in wastewater using neodymium doped polyaniline supported layered double hydroxide nanocomposite, J. Hazard. Mater. 416 (2021) 125754-125765. https://doi.org/10.1016/j.jhazmat.2021.125754.
[71] T.-Y. Chi, Z. Chen, J. Kameoka, Perfluorooctanesulfonic Acid Detection Using Molecularly Imprinted Polyaniline on a Paper Substrate, Sensors. 20 (2020) 7301-7315. https://doi.org/10.3390/s20247301.
[72] C. Fang, Z. Chen, M. Megharaj, R. Naidu, Potentiometric detection of AFFFs based on MIP, Environ. Technol. Innov. 5 (2016) 52–59. https://doi.org/10.1016/j.eti.2015.12.003.
[73] J. Gong, T. Fang, D. Peng, A. Li, L. Zhang, A highly sensitive photoelectrochemical detection of perfluorooctanic acid with molecularly imprined polymer-functionalized nanoarchitectured hybrid of AgI–BiOI composite, Biosens. Bioelectron. 73 (2015) 256–263. https://doi.org/10.1016/j.bios.2015.06.008.

[74] X. Li, X. Wang, T. Fang, L. Zhang, J. Gong, Disposable photoelectrochemical sensing strip for highly sensitive determination of perfluorooctane sulfonyl fluoride on functionalized screen-printed carbon electrode, Talanta. 181 (2018) 147–153. https://doi.org/10.1016/j.talanta.2018.01.005.
[75] T. Tran.T, J. Li, H. Feng, J. Cai, L. Yuan, N. Wang, Q. Cai, Molecularly imprinted polymer modified TiO2 nanotube arrays for photoelectrochemical determination of perfluorooctane sulfonate (PFOS), Sens. Actuators B Chem. 190 (2014) 745–751. https://doi.org/10.1016/j.snb.2013.09.048.
[76] S. Chen, A. Li, L. Zhang, J. Gong, Molecularly imprinted ultrathin graphitic carbon nitride nanosheets–Based electrochemiluminescence sensing probe for sensitive detection of perfluorooctanoic acid, Anal. Chim. Acta. 896 (2015) 68–77. https://doi.org/10.1016/j.aca.2015.09.022.
[77] H. Feng, N. Wang, T. Tran.T, L. Yuan, J. Li, Q. Cai, Surface molecular imprinting on dye–(NH2)–SiO2 NPs for specific recognition and direct fluorescent quantification of perfluorooctane sulfonate, Sens. Actuators B Chem. 195 (2014) 266–273. https://doi.org/10.1016/j.snb.2014.01.036.
[78] Z. Jiao, J. Li, L. Mo, J. Liang, H. Fan, A molecularly imprinted chitosan doped with carbon quantum dots for fluorometric determination of perfluorooctane sulfonate, Microchim. Acta. 185 (2018) 473-481. https://doi.org/10.1007/s00604-018-2996-y.
[79] L. Zheng, Y. Zheng, Y. Liu, S. Long, L. Du, J. Liang, C. Huang, M.T. Swihart, K. Tan, Core-shell quantum dots coated with molecularly imprinted polymer for selective photoluminescence sensing of perfluorooctanoic acid, Talanta. 194 (2019) 1–6. https://doi.org/10.1016/j.talanta.2018.09.106.
[80] N. Cennamo, G. D'Agostino, G. Porto, A. Biasiolo, C. Perri, F. Arcadio, L. Zeni, A Molecularly Imprinted Polymer on a Plasmonic Plastic Optical Fiber to Detect Perfluorinated Compounds in Water, Sensors. 18 (2018) 1836-1846. https://doi.org/10.3390/s18061836.
[81] W.-W. Zhao, M. Xiong, X.-R. Li, J.-J. Xu, H.-Y. Chen, Photoelectrochemical bioanalysis: A mini review, Electrochem. Commun. 38 (2014) 40–43. https://doi.org/10.1016/j.elecom.2013.10.035.
[82] W.-W. Zhao, J.-J. Xu, H.-Y. Chen, Photoelectrochemical bioanalysis: the state of the art, Chem. Soc. Rev. 44 (2015) 729–741. https://doi.org/10.1039/C4CS00228H.
[83] L. Shi, Y. Yin, L.-C. Zhang, S. Wang, M. Sillanpää, H. Sun, Design and engineering heterojunctions for the photoelectrochemical monitoring of environmental pollutants: A review, Appl. Catal. B Environ. 248 (2019) 405–422. https://doi.org/10.1016/j.apcatb.2019.02.044.
[84] K. Fähnrich, M. Pravda, G. G Guilbault, Recent applications of electrogenerated chemiluminescence in chemical analysis, Talanta. 54 (2001) 531–559. https://doi.org/10.1016/S0039-9140(01)00312-5.
[85] L. Hu, G. Xu, Applications and trends in electrochemiluminescence, Chem. Soc. Rev. 39 (2010) 3275-3304. https://doi.org/10.1039/b923679c.
[86] L. Cumba, Y. Pellegrin, F. Melinato, R.J. Forster, Enhanced Electrochemiluminescence from 3D Nanocavity Electrode Arrays, Sens. Actuators Rep. 4 (2022) 100082-100087. https://doi.org/10.1016/j.snr.2022.100082.
[87] N.P. Sardesai, J.C. Barron, J.F. Rusling, Carbon Nanotube Microwell Array for Sensitive Electrochemiluminescent Detection of Cancer Biomarker Proteins, Anal. Chem. 83 (2011) 6698–6703. https://doi.org/10.1021/ac201292q.
[88] H. Yu, J.G. Bruno, Immunomagnetic-electrochemiluminescent detection of Escherichia coli O157 and Salmonella typhimurium in foods and environmental water samples, Appl. Environ. Microbiol. 62 (1996) 587–592. https://doi.org/10.1128/aem.62.2.587-592.1996.
[89] G. Jie, L. Li, C. Chen, J. Xuan, J.-J. Zhu, Enhanced electrochemiluminescence of CdSe quantum dots composited with CNTs and PDDA for sensitive immunoassay, Biosens. Bioelectron. 24 (2009) 3352–3358. https://doi.org/10.1016/j.bios.2009.04.039.
[90] P. Rebelo, E. Costa-Rama, I. Seguro, J.G. Pacheco, H.P.A. Nouws, M.N.D.S. Cordeiro, C. Delerue-Matos, Molecularly imprinted polymer-based electrochemical sensors for environmental analysis, Biosens. Bioelectron. 172 (2021) 112719-112736. https://doi.org/10.1016/j.bios.2020.112719.
[91] K. Risha, J. Flaherty, R. Wille, W. Buck, F. Morandi, T. Isemura, Method for Trace Level Analysis of C8, C9, C10, C11, and C13 Perfluorocarbon Carboxylic Acids in Water, Anal. Chem. 77 (2005) 1503–1508. https://doi.org/10.1021/ac0490548.

[92] C. Capolungo, D. Genovese, M. Montalti, E. Rampazzo, N. Zaccheroni, L. Prodi, Photoluminescence-Based Techniques for the Detection of Micro- and Nanoplastics, Chem. – Eur. J. 27 (2021) 17529–17541. https://doi.org/10.1002/chem.202102692.
[93] D.T. McQuade, A.E. Pullen, T.M. Swager, Conjugated Polymer-Based Chemical Sensors, Chem. Rev. 100 (2000) 2537–2574. https://doi.org/10.1021/cr9801014.
[94] X. Sun, Y. Lei, Fluorescent carbon dots and their sensing applications, TrAC Trends Anal. Chem. 89 (2017) 163–180. https://doi.org/10.1016/j.trac.2017.02.001.
[95] B. Qu, J. Sun, P. Li, L. Jing, Current advances on g-C3N4-based fluorescence detection for environmental contaminants, J. Hazard. Mater. 425 (2022) 127990-128007. https://doi.org/10.1016/j.jhazmat.2021.127990.
[96] R. Gui, H. Jin, Recent advances in synthetic methods and applications of photo-luminescent molecularly imprinted polymers, J. Photochem. Photobiol. C Photochem. Rev. 41 (2019) 100315-100352. https://doi.org/10.1016/j.jphotochemrev.2019.08.002.
[97] V. Hodnik, G. Anderluh, Toxin Detection by Surface Plasmon Resonance, Sensors. 9 (2009) 1339–1354. https://doi.org/10.3390/s9031339.
[98] Y. Wang, T.-X. Wei, Surface plasmon resonance sensor chips for the recognition of bovine serum albumin via electropolymerized molecularly imprinted polymers, Chin. Chem. Lett. 24 (2013) 813–816. https://doi.org/10.1016/j.cclet.2013.05.004.
[99] Y. Saylan, A. Denizli, Molecular Fingerprints of Hemoglobin on a Nanofilm Chip, Sensors. 18 (2018) 3016-3028. https://doi.org/10.3390/s18093016.
[100] G. Ertürk, H. Özen, M.A. Tümer, B. Mattiasson, A. Denizli, Microcontact imprinting based surface plasmon resonance (SPR) biosensor for real-time and ultrasensitive detection of prostate specific antigen (PSA) from clinical samples, Sens. Actuators B Chem. 224 (2016) 823–832. https://doi.org/10.1016/j.snb.2015.10.093.
[101] R. Verma, B.D. Gupta, Optical fiber sensor for the detection of tetracycline using surface plasmon resonance and molecular imprinting, The Analyst. 138 (2013) 7254-7263. https://doi.org/10.1039/c3an01098h.
[102] N. Cennamo, G. D'Agostino, R. Galatus, L. Bibbò, M. Pesavento, L. Zeni, Sensors based on surface plasmon resonance in a plastic optical fiber for the detection of trinitrotoluene, Sens. Actuators B Chem. 188 (2013) 221–226. https://doi.org/10.1016/j.snb.2013.07.005.
[103] H. Agrawal, A.M. Shrivastav, B.D. Gupta, Surface plasmon resonance based optical fiber sensor for atrazine detection using molecular imprinting technique, Sens. Actuators B Chem. 227 (2016) 204–211. https://doi.org/10.1016/j.snb.2015.12.047.
[104] A.M. Shrivastav, S.P. Usha, B.D. Gupta, Fiber optic profenofos sensor based on surface plasmon resonance technique and molecular imprinting, Biosens. Bioelectron. 79 (2016) 150–157. https://doi.org/10.1016/j.bios.2015.11.095.
[105] N. Cennamo, L. Zeni, P. Tortora, M.E. Regonesi, A. Giusti, M. Staiano, S. D'Auria, A. Varriale, A High Sensitivity Biosensor to detect the presence of perfluorinated compounds in environment, Talanta. 178 (2018) 955–961. https://doi.org/10.1016/j.talanta.2017.10.034.
[106] N. Cennamo, G. D'Agostino, F. Sequeira, F. Mattiello, G. Porto, A. Biasiolo, R. Nogueira, L. Bilro, L. Zeni, A Simple and Low-Cost Optical Fiber Intensity-Based Configuration for Perfluorinated Compounds in Water Solution, Sensors. 18 (2018) 3009-3019. https://doi.org/10.3390/s18093009.